Journal of Biosystems Engineering (2019) 44:103–111
https://doi.org/10.1007/s42853-019-00012-2

Online ISSN 2234-1862
Print ISSN 1738-1266

ORIGINAL ARTICLE

Substrate Mixture Optimization of Nutrients Needed for Methane Yield

Peter Tumutegyereize[1] · Clever Ketlogetswe[2] · Jerekias Gandure[2] · Noble Banadda[1]

Received: 15 January 2019 / Revised: 7 March 2019 / Accepted: 7 March 2019 / Published online: 12 April 2019

Abstract

Purpose The twofold aim of this study was to optimize nutrients important for methane yield in substrate mixtures and to assess the effect of the optimized nutrients on methane production.

Method Augmented simplex lattice design was used on three substrates, i.e., matooke peels (MPs), cassava peels (CPs), and sweet potato peels (SPs) wherein 16 ratio combinations were assessed for their macro- and micronutrient compositions and methane production potential. Experimental data was simulated using canonical polynomial models to determine mixture combinations with optimal nutrients stimulatory to methane yield.

Results Six optimization solutions with the global optimal having a desirability of 0.93 and a ratio of 0.611:0.375:0.015 were observed to be localized over the design space. Biomethane experiments were in agreement with the optimized mixture ratios as ratios that gave the highest methane yield of 0.3 Nm^3CH_4/kg VS and above lay in the optimized design region.

Conclusion Therefore, charts showing optimized regions of different substrate mixtures in terms of their nutrients can be a tool in biogas digester operations.

Keywords Substrate mixtures · Nutrients · Anaerobic digestion · Polynomial models · Methane

Introduction

Both macro- and micronutrients have been reported to enhance methane production (Demirel and Scherer 2011; Pobeheim et al. 2010; Schattauer et al. 2011); however, in contrast, they can be inhibitors or toxic to the methane formation process (Appels et al. 2008; Chen et al. 2008). In addition, single substrates are said to be imbalanced in terms of nutrients when used as biogas substrates (Li et al. 2013). One possible solution to this nutrient imbalance is co-digestion or mixing two or more substrates together (Garcia-Peña et al. 2011; Krishania et al. 2013; Li et al. 2013; Macias-Corral et al. 2008; Marañón et al. 2012; Zaher et al. 2009). The challenge, however, is getting the second or third substrate for co-digestion without incurring extra costs in terms of transport or purchasing which reduces the net energy benefit of the project (Berglund and Börjesson 2006; Walla and Schneeberger 2008). Different researchers have proposed concentration limits of different nutrients that are stimulatory to methane yield without inhibition as presented in Table 1.

At a household level, however, the waste generated is of mixed composition depending on the eating habits of a given household/community. In this mixed composition, particular constituents stand out most of the time, if not on a daily basis. Little attention has been paid to these waste constituents in the mixture as far as their influence on biogas/methane production is concerned. Yet, inhibition of methane formation is dependent on the proportion of different substrates in the mixture and not on the total amount of substrates (Álvarez et al. 2010). Instead, researchers have continued considering household waste wholesomely as a single substrate for biogas

✉ Peter Tumutegyereize
pierretumutegye@gmail.com

Clever Ketlogetswe
ketloget@ub.ac.bw

Jerekias Gandure
Ganduretj@ub.ac.bw

Noble Banadda
banadda@caes.mak.ac.ug

[1] Department of Agricultural and Biosystems Engineering, Makerere University, P.O. Box 7062, Kampala, Uganda

[2] Department of Mechanical Engineering, University of Botswana, Private Bag 0061, Gaborone, Botswana

Table 1 Concentration limits of mineral nutrients that are not inhibitory to methane production

Mineral nutrient	Concentration limit (mg/kg)	References
Ca	200–7000	(Appels et al. 2008; Chen et al. 2008)
K	≤ 2500	(Appels et al. 2008)
Na	350	(Appels et al. 2008)
Mg	75–4800	(Appels et al. 2008; Schattauer et al. 2011)
Al	≤ 2500	(Chen et al. 2008)
Fe	0.28–50.4	(Schattauer et al. 2011)
Mn	0.005–55	
Cu	0.06–64	
Co	0.00059–0.19	
Ni	0.0059–5	
S	0.32–13,000	
Pb	0.02–200	

production, and the results have not been promising. Therefore, continuing to take household waste as a single substrate without taking into account the different constituent proportions totally disregards the factors that inhibit methane formation. Hence, there is a need to understand nutrient levels and influence of the household waste constituents in varying mixed proportions on the methane yield.

In Uganda, for example, matooke peels (MPs), i.e., peels from the East African Highland's cooking-type banana, cassava peels (CPs), and sweet potato peels and vines (SPs) are agricultural wastes that are widely common in people's homes. These three wastes are not only present in Uganda but also in most developing countries as they originate from their main staple foods (Katongole et al. 2011; Kinobe et al. 2015). The disposal of these wastes is a challenge especially in the urban areas given that approximately 60% of municipal solid waste (MSW) comes from households (Fehr et al. 2000; Hanc et al. 2011; Ogwueleka 2013) and over 90% of MSW is organic (Komakech et al. 2014). Although some people (approximately 65%) with animals often collect these wastes as animal feeds (Katongole et al. 2011), their efforts are negligible given that they mainly use them during the dry season (Mabala 2015). This has made matooke peels the common wastes at landfills (Kinobe et al. 2015). In contrast, MPs are being used for making briquette. However, the unit cost of energy from briquettes in Uganda has been found to be more than twice that of charcoal, thereby making briquettes unattractive to charcoal users (Tumutegyereize et al. 2016).

Therefore, the aim of our study is to assess the effect of substrate mixtures of MP, CP, and SP on nutrients important for biogas production and to optimize mixtures before they are subjected to anaerobic co-digestion. This is in light of the fact that MPs, for example, are considered to have considerable amounts of potassium (Komakech et al. 2014) which has the potential of neutralizing the membrane potential of anaerobic microorganisms as well as extracts other metals bound to exchangeable sites in any mixture (Chen et al. 2008). Therefore, mixing MP, CP, and SP together would have an antagonizing or synergizing effect owing to the combination of other elements on the high or low levels of any nutrient in the mixture. For example, a combination of sodium, magnesium, ammonium, and calcium is said to have a moderating effect on high levels of potassium (Appels et al. 2008; Chen et al. 2008). In this manner, methane inhibition due to micro- and macronutrients can be controlled or minimized. More so, these nutrients are expected to be supplied by the substrate, thus making the selection of the substrate extremely critical in the abundance of nutrients (Schattauer et al. 2011). In this regard, nutrients are no longer regarded a scientific anomaly but an engineering necessity (Speece 1996). According to Demirel and Scherer (2011), the lack or imbalance of these nutrients in biogas digesters is probably the first cause of process inefficiency despite proper management and control of other operational and environmental parameters.

Materials and Methods

Sample Preparation

Samples were prepared following the AOAC (2006) standard method for the preparation of laboratory samples of plant origin. Samples of MP, CP, and SP that are free from any foreign matter were secured through buying matooke, cassava, and sweet potato from the local markets in Kampala, peeled, air-dried, and grinded using a laboratory mill (Christy Hunt Agricultural Limited, Machine type 8″, Serial No. 24387) at the Makerere University Agricultural Research Institute Kabanyolo (MUARIK) and packed in air-tight bags ready for analysis.

Experimental Design

An augmented simplex lattice design (ASLD) was used for designing the experiment given that methane formation inhibition is dependent on the proportion of different substrates in the mixture (Álvarez et al. 2010). That is to say, according to Cornell (2002), a [q, m] simplex lattice design for q components will have design points given as

$$\binom{q+m-1}{m} = {}^{(q+m-1)!}/_{m!(q-1)!},$$

where m denotes the number of equal spacing between the proportions assumed by each component to take $m + 1$ values from 0 to 1, that is, $x_i = 0, {}^1/_m, {}^2/_m, ..., 1$ for $i = 1, 2, ..., q$. Therefore, the design is restricted by Eq. 1. Due to this restriction, the polynomial model that can be used to fit the data corresponding to the design points is different from the traditional polynomial. Instead, it is called the canonical polynomial which can be linear, quadratic, special quadratic, cubic, or special cubic. Presented in Eqs. 2, 3, and 4 are the linear, quadratic, and special cubic canonical polynomial models used to fit to the data from a mixture experiment.

$$\sum_{i=1}^{q} x_i = x_1 + x_2 + ... + x_q = 1.0 \quad (1)$$

$$\eta = \sum_{i=1}^{q} \beta_i x_i \quad (2)$$

$$\eta = \sum_{i=1}^{q} \beta_i x_i + \sum_{i=1}^{q} \sum_{i<j}^{q} \beta_{ij} x_i x_j \quad (3)$$

$$\eta = \sum_{i=1}^{q} \beta_i x_i + \sum_{i=1}^{q} \sum_{i<j}^{q} \beta_{ij} x_i x_j + \sum_{k=1}^{q} \sum_{j<k}^{q} \sum_{i<j}^{q} \beta_{ijk} x_i x_j x_k \quad (4)$$

where

η is the expected response at any design point

β_i is the effect on the response of changing the proportion of component *i*

β_{ij} is the effect on the response of changing the proportions of any two components

β_{ijk} is the effect on the response of changing the proportions of all components

Ratios of MP:CP:SP were the variables while K, Na, Ca, Mg, Zn, Co, Al, Cu, Mn, Pb, Ni, S, and Fe were the responses. A total of 16 sample ratios were analyzed as shown in Table 2.

Instrumentation

Microwave plasma-atomic emission spectrometry (4100 MP-AES, Agilent, Santa Clara, CA, USA) was used for the determination of Zn, Co, Al, Cu, Mn, Pb, Ni, and Fe. The viewing position and nebulizer pressures were optimized automatically using the Agilent MP Expert software version 1.1.1.45895. Magnesium was determined using atomic absorption spectrometry (AAS), while Na, Ca, and K were determined using a flame atomic emission spectrometry. Nitrous oxide-acetylene flame was used for Ca due to its high temperature compared to the air-acetylene flame used for Mg, Na, and K to avoid chemical interference due to phosphates. In contrast, sulfur was determined using a S-144DR sulfur determinator by the infrared detection method with an oven temperature of 48.38 °C, furnace temperature of 1220.32 °C, furnace set point of 1253.20 °C, and both pump/oxygen inlet and incoming pressure on. Zn, Co, Al, Cu, Mn, Pb, Ni, Fe, Na, Ca, K, Mg, and S were all determined according to AOAC (2000). Biomethane potential was determined using 250-mL serum bottles with a working volume of 150 mL following the procedures described by Angelidaki et al. (2009) and Hansen et al. (2004).

Analysis and Optimization

Design Expert 7.0 (trial version), a statistical package, was used for regression analysis and optimization. Global and local optimum ratios that would give nutrient concentrations that are not inhibitory but stimulatory to methane production were achieved by setting targets for K, Na, Mn, and Cu, maximizing Mg and minimizing S, while Ca, Co, and Ni were kept within the range. This was based on concentration limits of different nutrients that are said to not cause deficiency or an inhibitory effect on methane production already presented in Table 1.

Sample Preparation for MP-AES and AAS Analyses

Sample solutions for metal analysis were prepared by the dry ashing standard method. For this, 1 g of each dried and ground sample was weighed into a porcelain crucible and then ashed for 2 h at 500 °C. However, the furnace was set at 520 °C since at 500 °C, it would be less by 20 °C as detected by the K-type thermocouple. After ashing for 2 h, the crucibles were cooled in a desiccator and 10 drops (approximate to 0.5 mL) of deionized water from a Millipore system added followed by 4 mL of HNO_3 with 50% dilution. Crucibles were then heated on a hot plate at 120 °C to evaporate excess HNO_3 and placed in the furnace for 1 h at 500 °C. After cooling the crucibles, the ash was dissolved in 10 mL of HCl with 50% dilution and the content was transferred to a 100-mL volumetric flask where it was diluted to volume by deionized water (AOAC 2006).

Results and Discussion

Effect of Substrate Mixtures on Nutrients

Table 2 shows the experimental means for the analyzed nutrients against MP:CP:SP ratios. Generally, Na and Cu could not be detected in ratios without MP while Co could not be detected as MP was introduced in the ratios. Table 2 may not explain the effect of ratios on the different nutrients well, despite large decreases or increases in concentrations as ratios changed. Therefore, regression models and response surfaces were generated to explain this effect. The relationships between Ca, K, Na, Mg, Fe, Al, Zn, Cu, and S and MP:CP:SP ratios were observed to be best predicted by cubic regressional models significant at a 95% confidence level. This is contrary to the default

Table 2 Experimental design and average means for the analyzed mineral nutrients

Substrate ratios			Average means of mineral nutrients (mg/kg DM)												
MP	CP	SP	Ca	K	Mg	Na	Fe	Al	Zn	Co	Mn	Cu	Ni	Pb	S
0.00	0.00	1.00	394.08	1331.78	53.89	N.D	3643.39	8278.99	78.03	2.03	480.12	349.17	5.00	14.56	1919.30
0.00	0.50	0.50	212.86	508.39	13.22	N.D	3350.20	7209.54	11.96	2.70	331.26	N.D	0.83	11.42	2302.95
0.00	0.33	0.67	N.D	675.10	13.11	N.D	4762.48	7994.18	30.19	1.20	380.74	N.D	9.17	12.08	2063.10
0.00	0.67	0.33	90.16	498.06	9.88	N.D	5135.09	9364.24	90.73	0.35	347.96	N.D	3.83	10.89	2153.70
0.00	1.00	0.00	N.D	145.15	N.D	N.D	3145.09	5667.49	66.96	1.30	141.62	N.D	2.25	4.96	2035.20
0.50	0.00	0.50	1838.20	2915.94	152.80	141.73	3488.68	7198.08	47.24	1.80	310.04	N.D	0.50	13.93	1560.10
0.33	0.00	0.67	2203.18	2697.54	176.49	763.19	2977.18	6640.13	14.89	1.20	354.21	N.D	0.75	14.66	2120.60
0.50	0.50	0.00	2369.69	2460.52	184.55	1265.08	2593.41	5132.37	86.08	0.50	73.68	N.D	2.17	13.34	1959.05
0.33	0.33	0.33	2340.62	2307.64	176.38	957.02	3552.22	7572.74	82.51	N.D	360.34	50.83	3.75	12.91	1848.95
0.167	0.167	0.67	1989.73	1977.21	159.98	518.07	3103.58	6473.06	46.31	N.D	217.09	N.D	0.50	12.00	2445.75
0.33	0.67	0.00	2047.49	1515.33	160.31	765.35	2544.77	5036.62	46.47	N.D	78.41	48.33	0.83	9.27	2168.15
0.167	0.67	0.167	2366.24	1381.88	177.39	797.24	3052.66	6074.72	72.95	N.D	129.95	88.75	1.00	13.91	1893.55
0.67	0.00	0.33	2245.98	3352.34	172.97	1050.74	2481.06	5589.42	45.09	N.D	190.11	130.33	0.50	10.53	1742.10
0.67	0.33	0.00	54,857.32	4699.89	376.72	N.D	2019.61	4065.87	61.73	N.D	11.92	20.50	0.75	14.50	1137.92
0.67	0.167	0.167	2066.23	2704.98	164.59	98.99	5402.90	5362.16	122.46	N.D	6.76	399.17	N.D	15.02	1332.20
1.00	0.00	0.00	47,291.12	166,068.75	178.05	261.40	3951.89	6373.55	111.17	N.D	N.D	475.25	1.50	16.70	1153.45

N.D, not detected

linear relationship most literature seem to suggest (Macias-Corral et al. 2008; Heo et al. 2004). Figure 1 a–i illustrate the behavior of these responses (nutrients) over the design space, and Eqs. 5–13 show the cubic models describing their relationships. Only the cubic regressional model for Fe explained less than 50% ($R^2 = 0.48$) of the captured response variability. However, it still described the relationship between the significant MP:CP:SP ratios and Fe as it was significant (P value = 0.0015) with an adequate signal-to-noise ratio of 6.6 which is greater than 4, the minimum (Table 3). This can also be said of the models for Co, Ni, and Pb whose R^2 values were less than 0.5.

$$\mathrm{Ca} = 7909.23 \times \mathrm{MP} - 9113.67 \times \mathrm{MP} \times \mathrm{SP} + 11801.61 \times \mathrm{MP} \times \mathrm{CP} \times (\mathrm{MP} - \mathrm{CP}) - 25387.64 \times \mathrm{MP} \times \mathrm{SP} \times (\mathrm{MP} - \mathrm{SP}) \quad (5)$$

$$\mathrm{In}(K) = 12.02 \times \mathrm{MP} + 4.98 \times \mathrm{CP} + 7.19 \times \mathrm{SP} - 2.76 \times \mathrm{MP} \times \mathrm{CP} - 6.81 \times \mathrm{MP} \times \mathrm{SP} + 1.08 \times \mathrm{CP} \times \mathrm{SP} + 15.66 \times \mathrm{MP} \times \mathrm{CP} \times \mathrm{SP} - 10.04 \times \mathrm{MP} \times \mathrm{CP} \times (\mathrm{MP} - \mathrm{CP}) - 10.24 \times \mathrm{MP} \times \mathrm{SP} \times (\mathrm{MP} - \mathrm{SP}) + 3.25 \times \mathrm{CP} \times \mathrm{SP} \times (\mathrm{CP} - \mathrm{SP}) \quad (6)$$

$$\mathrm{Mg} = 189.65 \times \mathrm{MP} + 56.38 \times \mathrm{SP} + 621.20 \times \mathrm{MP} \times \mathrm{CP} + 204.58 \times \mathrm{MP} \times \mathrm{SP} + 684.57 \times \mathrm{MP} \times \mathrm{CP} \times \mathrm{SP} - 650.45 \times \mathrm{MP} \times \mathrm{SP} \times (\mathrm{MP} - \mathrm{SP}) \quad (7)$$

$$\mathrm{Na} = +2465.92 \times \mathrm{MP} \times \mathrm{CP} + 2232.98 \times \mathrm{MP} \times \mathrm{SP} - 7366.81 \times \mathrm{MP} \times \mathrm{CP} \times (\mathrm{MP} - \mathrm{CP}) \quad (8)$$

$$\mathrm{Fe} = -4204.68 \times \mathrm{MP} \times \mathrm{CP} + 3839.35 \times \mathrm{CP} \times \mathrm{SP} + 25547.16 \times \mathrm{MP} \times \mathrm{CP} \times \mathrm{SP} \quad (9)$$

$$\mathrm{Al} = 6267.99 \times \mathrm{MP} + 5701.91 \times \mathrm{CP} + 8303.53 \times \mathrm{SP} - 5348.28 \times \mathrm{MP} \times \mathrm{CP} - 3226.64 \times \mathrm{MP} \times \mathrm{SP} + 4594.96 \times \mathrm{CP} \times \mathrm{SP} + 12134.70 \times \mathrm{CP} \times \mathrm{SP} \times (\mathrm{CP} - \mathrm{SP}) \quad (10)$$

$$\mathrm{In(Zn)} = 4.80 \times \mathrm{MP} + 4.21 \times \mathrm{CP} + 4.54 \times \mathrm{SP} - 5.25 \times \mathrm{MP} \times \mathrm{SP} - 3.49 \times \mathrm{CP} \times \mathrm{SP} + 32.57 \times \mathrm{MP} \times \mathrm{CP} \times \mathrm{SP} + 6.66 \times \mathrm{MP} \times \mathrm{SP} \times (\mathrm{MP} - \mathrm{SP}) + 5.51 \times \mathrm{CP} \times \mathrm{SP} \times (\mathrm{CP} - \mathrm{SP}) \quad (11)$$

$$\mathrm{Cu} = 413.59 \times \mathrm{MP} + 358.30 \times \mathrm{SP} - 762.34 \times \mathrm{MP} \times \mathrm{CP} - 1446.75 \times \mathrm{MP} \times \mathrm{SP} - 803.36 \times \mathrm{CP} \times \mathrm{SP} + 5204.40 \times \mathrm{MP} \times \mathrm{CP} \times \mathrm{SP} + 1390.86 \times \mathrm{MP} \times \mathrm{SP} \times (\mathrm{MP} - \mathrm{SP}) + 918.31 \times \mathrm{CP} \times \mathrm{SP} \times (\mathrm{CP} - \mathrm{SP}) \quad (12)$$

$$\mathrm{S} = 1144.74 \times \mathrm{MP} + 1999.93 \times \mathrm{CP} + 1918.82 \times \mathrm{SP} + 1279.92 \times \mathrm{MP} \times \mathrm{SP} + 915.43 \times \mathrm{CP} \times \mathrm{SP} - 3951.81 \times \mathrm{MP} \times \mathrm{CP} \times (\mathrm{MP} - \mathrm{CP}) - 1899.83 \times \mathrm{MP} \times \mathrm{SP} \times (\mathrm{MP} - \mathrm{SP}) \quad (13)$$

Nickel and cobalt were best predicted by the quadratic model (Eq. 14) and the special cubic regression model (Eq. 15), respectively. Figure 2 a and b show the response surfaces of Ni and Co over the design space, respectively.

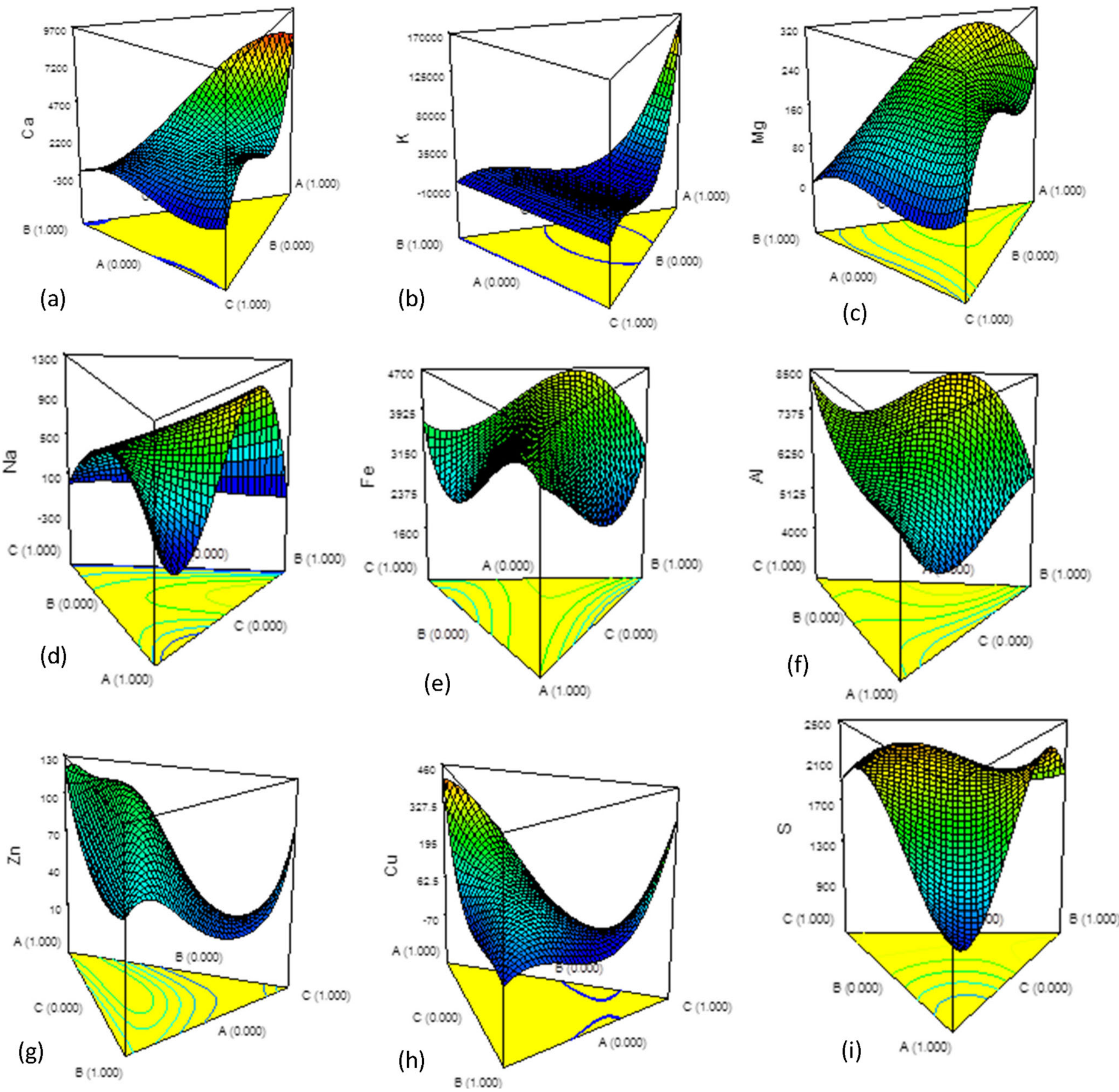

Fig. 1 Cubic response surfaces for Ca, K, Mg, Na, Fe, Al, Zn, Cu, and S

Table 3 Models' coefficients of determination

	Ca	K	Mg	Na	Fe	Al	Zn	Co	Mn	Cu	Ni	Pb	S
Model *P* value	< 0.0001	< 0.0001	< 0.0001	< 0.0001	0.0015	< 0.0001	< 0.0001	0.0007	< 0.0001	< 0.0001	0.0002	< 0.0001	< 0.0001
R^2	0.84	1.00	0.84	0.65	0.48	0.79	0.66	0.42	0.81	0.82	0.43	0.42	0.81
Adj R^2	0.80	0.99	0.80	0.56	0.36	0.74	0.58	0.34	0.81	0.78	0.36	0.39	0.77
Pred R^2	0.76	0.99	0.76	0.49	0.22	0.69	0.51	0.22	0.80	0.72	0.28	0.32	0.72
Adeq precision	16.04	140.81	14.91	8.63	6.63	12.60	8.87	6.83	30.30	14.61	8.61	12.64	13.18

$$\text{Ni} = 2.65 \times \text{CP} + 4.66 \times \text{SP} - 10.87 \times \text{MP} \times \text{SP} \quad (14)$$

$$\text{Co} = 1.07 \times \text{CP} + 1.53 \times \text{SP} - 29.20 \times \text{MP} \times \text{CP} \times \text{SP} \quad (15)$$

Manganese and lead were best predicted by linear regression models in Eqs. 16 and 17 with their visual illustrations in Fig. 2 c and d, respectively. It should be noted that terms that were significant but with confidence intervals spanning from negative to positive were omitted from the models. This is because their coefficients could probably be zero indicating that such a term may not have a statistically significant effect on the response. From Figs. 1 and 2, we can infer that as one moves away from any apex of the design space that represents a pure substrate, the response surface changes in color, signifying change in concentration of any nutrient at hand. Therefore, the changes in color of the response surfaces over the design space demonstrate the effect of mixing the three substrates on nutrient concentrations. This suggests that these models can be used to formulate substrate ratios with the recommended nutrient concentrations critical for methane production before anaerobic digestion. Therefore, researchers have developed databases for a number of the common substrates used as a basis of reference in biogas production in terms of their biomethane potential (Gunaseelan 1997). Efforts to develop a database of nutrient composition of common substrate mixtures stimulatory to methane yield would be necessary for biogas operators. It is also important to note that there are other factors that would render nutrients stimulatory or inhibitory to methane production like the chemical form of the element, pH, and redox potential (Chen et al. 2008), apart from the total concentration.

$$\text{Mn} = 144.52 \times \text{CP} + 499.24 \times \text{SP} \quad (16)$$

$$\text{Pb} = 16.54 \times \text{MP} + 9.38 \times \text{CP} + 13.48 \times \text{SP} \quad (17)$$

Mixture Optimization

Table 4 shows the optimization solutions with their desirability ranging from 0.928 as the global optimal to 0.686 for the local optimal solution. The six solutions that were predicted suggest that irrespective of which substrate material is more or less than the others among the three (MP, CP, and SP), it will always be possible to obtain an optimal ratio with the recommended nutrient concentrations that favor methane production. It should be noted that during optimization, Fe, Al, Pb, S, and Zn were not included. This is because Fe and Al concentrations were far above the recommended limits while Pb and S concentrations were within the limits for all ratios in the design, as shown in Table 2. However, the researchers could not find conclusive recommendations for Zn concentration needed for the methane yield. Figure 3 shows the regions on the design space where the optimal ratios having the recommended nutrient concentrations for methane production lay. The global optimal ratio can be seen to be 0.611:0.375:0.015 with a prediction (desirability) of 0.928. This is important because it can be used to test other substrates without

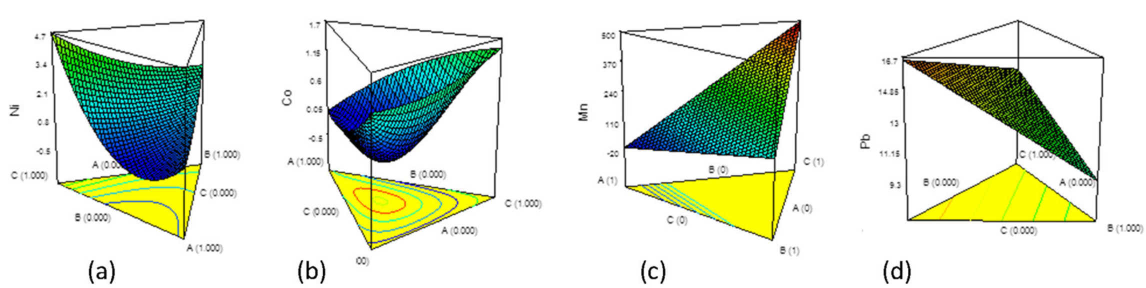

Fig. 2 Response surfaces for Ni, Co, Mn, and Pb

Table 4 Optimization solutions

No.	Optimum ratios			Mineral concentrations (mg/kg DM)								Desirability
	MP	CP	SP	Ca	K	Mg	Na	Co	Mn	Cu	Ni	
1	0.611	0.375	0.015	5611.716	3255.602	283.130	349.997	0.001	56.688	63.480	0.941	0.928
2	0.608	0.392	0.000	5743.556	3249.852	285.686	350.000	0.077	51.882	42.016	1.007	0.879
3	0.535	0.099	0.366	2192.100	2484.432	192.497	665.126	0.198	192.710	124.797	0.050	0.758
4	0.199	0.364	0.437	1672.061	1837.305	147.418	702.315	0.001	269.280	65.001	1.674	0.687
5	0.192	0.385	0.423	1626.134	1791.775	144.242	704.881	0.001	265.244	68.556	1.707	0.687
6	0.134	0.480	0.386	1287.844	1409.914	114.225	615.126	0.198	260.819	65.001	2.025	0.686

navigating the whole design space. Similarly, Fig. 4 shows the desirability response surface with the red color indicating the most desirable peak (0.93) over the design space.

Biomethane Potential

6 show cumulative specific methane yield from the tested substrate mixtures. It is generally shown that ratios of 0:1:1, 1:0:1, 2:0:1, 2:1:0, 1:1:1, and 1:1:4 plotted in Fig. 5 approximately lie in the optimized region shown in Fig. 3. These ratios also approximate the optimized ratios presented in Table 4. These ratios produced the highest specific methane yield of 0.3 Nm^3CH_4/kg VS and above. Their cumulative methane curves approximate to smooth curves which are expected in biomethane trial experiments. The generation of smooth cumulative methane curves implies that there was no process inhibition. On the contrary, cumulative methane curves in Fig. 6 exhibited anaerobic digestion process inhibition given that they are not smooth curves. It must be noted that most ratios in Fig. 6 do not lie in the optimal region. The difference between Figs. 5 and 6 can partly be attributed to the balanced nutrient composition in the substrate ratios plotted in Fig. 5, keeping other factors constant. This is an indication of

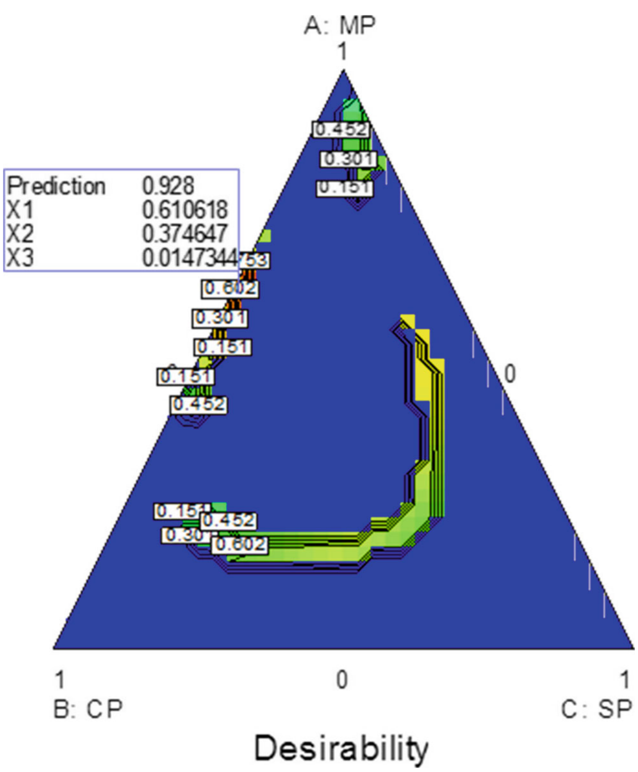

NB: X1 = MP; X2 = CP and X3= SP

Fig. 3 Contour plots over the design space showing regions of optimal ratios. NB: X1 = MP; X2 = CP, and X3 = SP

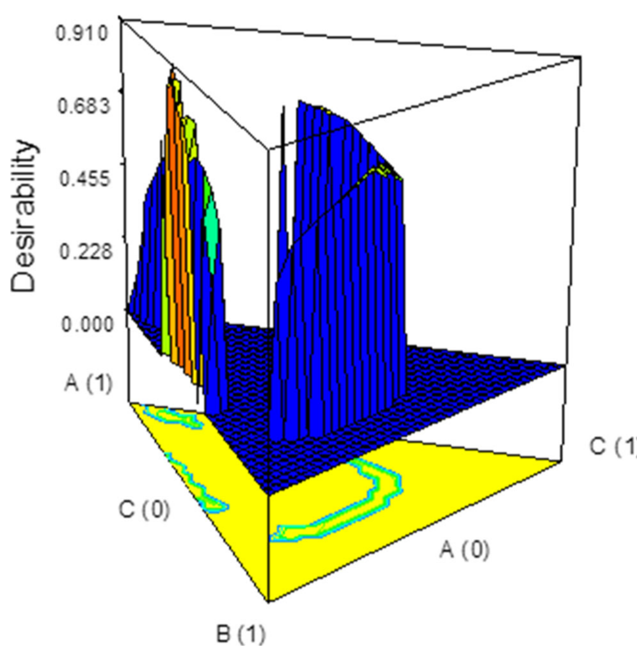

Fig. 4 Desirability response surface over the design space showing regions of optimal ratios

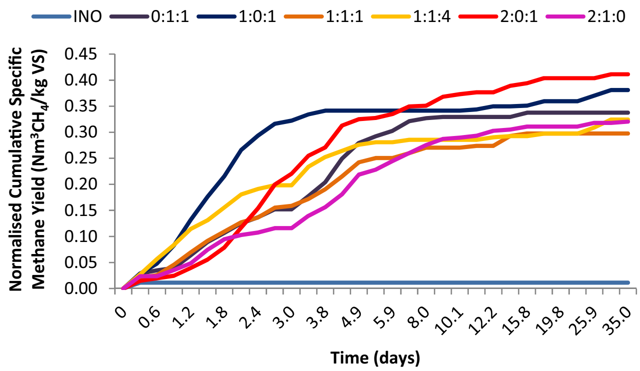

NB: INO represents inoculum

Fig. 5 Plot of normalized cumulative specific methane yield from the tested MP:CP:SP ratios that generated smooth curves. NB: INO represents inoculum

how important every fraction of any given substrate in a mixture is. These results also agree with the findings of Kim et al. (2017). Therefore, based on nutrient levels of substrate mixtures, the methane yield can be maximized. In addition, there are other factors like substrate origin and season, among others that were not part of the study, can influence nutrient levels and methane yield.

Conclusion

Results have demonstrated that the effect of mixing different substrates on nutrient concentrations does not follow a single trend. It follows cubic, special cubic, quadratic, and linear relationships for the different nutrients studied. Optimal ratios with the recommended concentration limits for methane production are not spread over the design space but localized. Biomethane potential results agreed with the optimized ratios as the highest specific volume of methane was attained from ratios that lay in the optimized region of the design space. Thus, charts showing regions of optimum nutrients of the common substrate mixtures would be a useful tool for biogas digester operators.

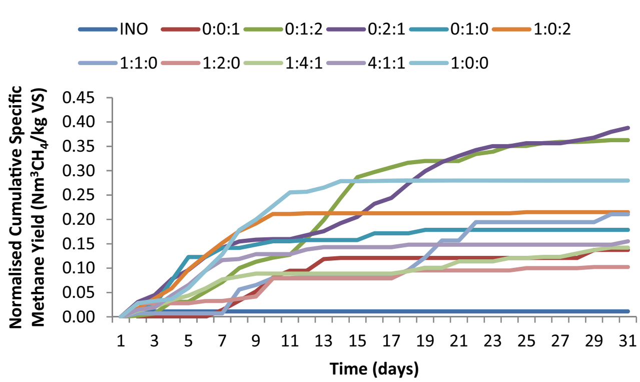

Fig. 6 Plot of cumulative specific methane yield from the tested MP:CP:SP ratios that failed to generate smooth curves

Funding Information Support for this research was made possible through a capacity building competitive grant *Training the next generation of scientists* provided by the Carnegie Cooperation of New York through the Regional Universities Forum for Capacity Building in Agriculture (RUFORUM) and Office of Research and Development (ORD) University of Botswana. Grant number: RU/2015/DFS/INTRA ACP/01

Compliance with Ethical Standards

Conflict of Interest The authors declare that they have no conflict of interests.

References

Álvarez, J., Otero, L., & Lema, J. (2010). A methodology for optimising feed composition for anaerobic co-digestion of agro-industrial wastes. *Bioresource Technology, 101*(4), 1153–1158.

Angelidaki, I., Alves, M., Bolzonella, D., Borzacconi, L., Campos, J., Guwy, A., ... Van Lier, J. (2009). Defining the biomethane potential (BMP) of solid organic wastes and energy crops: a proposed protocol for batch assays. *Water Science and Technology, 59*(5), 924–934.

AOAC (2006) (942.05). *Determination of ash in animal feed* (18th ed.). Gaitherburg: Association of Official Analytical Chemists International.

AOAC (2000) (985.01). *Metals and other elements in plants* (17th ed.). Gaitherburg: Association of Official Analytical Chemists International.

Appels, L., Baeyens, J., Degrève, J., & Dewil, R. (2008). Principles and potential of the anaerobic digestion of waste-activated sludge. *Progress in Energy and Combustion Science, 34*(6), 755–781. https://doi.org/10.1016/j.pecs.2008.06.002.

Berglund, M., & Börjesson, P. (2006). Assessment of energy performance in the life-cycle of biogas production. *Biomass and Bioenergy, 30*(3), 254–266.

Chen, Y., Cheng, J. J., & Creamer, K. S. (2008). Inhibition of anaerobic digestion process: a review. *Bioresource Technology, 99*(10), 4044–4064. https://doi.org/10.1016/j.biortech.2007.01.057.

Cornell, J. (2002). *Experiments with mixtures. Designs, models and the analysis of mixture data* (3rd ed.). New York: Wiley.

Demirel, B., & Scherer, P. (2011). Trace element requirements of agricultural biogas digesters during biological conversion of renewable biomass to methane. *Biomass and Bioenergy, 35*(3), 992–998. https://doi.org/10.1016/j.biombioe.2010.12.022.

Fehr, M., De Castro, M. S. M. V., & Calcado, M. D. R. (2000). A practical solution to the problem of household waste management in Brazil. *Resources, Conservation and Recycling, 30*(3), 245–257. https://doi.org/10.1016/S0921-3449(00)00063-X.

Garcia-Peña, E. I., Parameswaran, P., Kang, D. W., Canul-Chan, M., & Krajmalnik-Brown, R. (2011). Anaerobic digestion and co-digestion processes of vegetable and fruit residues: process and microbial ecology. *Bioresource Technology, 102*(20), 9447–9455. https://doi.org/10.1016/j.biortech.2011.07.068.

Gunaseelan, N. V. (1997). Anaerobic digestion of biomass for methane production: a review. *Biomass and Bioenergy, 13*(1–2), 83–114. https://doi.org/10.1016/S0961-9534(97)00020-2.

Hanc, A., Novak, P., Dvorak, M., Habart, J., & Svehla, P. (2011). Composition and parameters of household bio-waste in four seasons. *Waste Management, 31*(7), 1450–1460. https://doi.org/10.1016/j.wasman.2011.02.016.

Hansen, T. L., Schmidt, J. E., Angelidaki, I., Marca, E., Jansen, J. l. C., Mosbæk, H., & Christensen, T. H. (2004). Method for determination of methane potentials of solid organic waste. *Waste Management, 24*(4), 393–400. https://doi.org/10.1016/j.wasman.2003.09.009.

Heo, N. H., Park, S. C., & Kang, H. (2004). Effects of mixture ratio and hydraulic retention time on single-stage anaerobic co-digestion of food waste and waste activated sludge. *Journal of Environmental Science and Health, Part A, 39*(7), 1739–1756.

Katongole, C. B., Sabiiti, E., Bareeba, F., & Ledin, I. (2011). Utilization of market crop wastes as animal feed in urban and peri-urban livestock production in Uganda. *Journal of Sustainable Agriculture, 35*(3), 329–342.

Kim, M., Kim, S., & Kim, S. (2017). Effect of proximate composition ratios for biogas production. *Journal of Biosystems Engineering, 42*(3), 155–162. https://doi.org/10.5307/JBE.2017.42.3.155.

Kinobe, J. R., Gebresenbet, G., Niwagaba, C. B., & Vinnerås, B. (2015). Reverse logistics system and recycling potential at a landfill: a case study from Kampala City. *Waste Management, 42*, 82–92. https://doi.org/10.1016/j.wasman.2015.04.012.

Komakech, A. J., Banadda, N. E., Kinobe, J. R., Kasisira, L., Sundberg, C., Gebresenbet, G., & Vinneras, B. (2014). Characterization of municipal waste in Kampala, Uganda. *Journal of the Air & Waste Management Association (1995), 64*(3), 340–348.

Krishania, M., Kumar, V., Vijay, V. K., & Malik, A. (2013). Analysis of different techniques used for improvement of biomethanation process: a review. *Fuel, 106*, 1–9.

Li, Y., Zhang, R., Chen, C., Liu, G., He, Y., & Liu, X. (2013). Biogas production from co-digestion of corn stover and chicken manure under anaerobic wet, hemi-solid, and solid state conditions. *Bioresource Technology, 149*(0), 406–412. https://doi.org/10.1016/j.biortech.2013.09.091.

Mabala, R. (2015). *WhatsApp group inspired me into farming. Uganda Daily Monitor Newspaper*. Retrieved from https://www.monitor.co.ug/magazines/Farming/-whatsApp-group-inspired-me-into-farming-/689860-2837854-i5d3ygz/index.html.

Macias-Corral, M., Samani, Z., Hanson, A., Smith, G., Funk, P., Yu, H., & Longworth, J. (2008). Anaerobic digestion of municipal solid waste and agricultural waste and the effect of co-digestion with dairy cow manure. *Bioresource Technology, 99*(17), 8288–8293. https://doi.org/10.1016/j.biortech.2008.03.057.

Marañón, E., Castrillón, L., Quiroga, G., Fernández-Nava, Y., Gómez, L., & García, M. M. (2012). Co-digestion of cattle manure with food waste and sludge to increase biogas production. *Waste Management, 32*(10), 1821–1825. https://doi.org/10.1016/j.wasman.2012.05.033.

Ogwueleka, T. C. (2013). Survey of household waste composition and quantities in Abuja, Nigeria. *Resources, Conservation and Recycling, 77*, 52–60. https://doi.org/10.1016/j.resconrec.2013.05.011.

Pobeheim, H., Munk, B., Johansson, J., & Guebitz, G. M. (2010). Influence of trace elements on methane formation from a synthetic model substrate for maize silage. *Bioresource Technology, 101*(2), 836–839. https://doi.org/10.1016/j.biortech.2009.08.076.

Schattauer, A., Abdoun, E., Weiland, P., Plöchl, M., & Heiermann, M. (2011). Abundance of trace elements in demonstration biogas plants. *Biosystems Engineering, 108*(1), 57–65. https://doi.org/10.1016/j.biosystemseng.2010.10.010.

Speece, R. E. (1996). *Anarobic biotechnology for industrial wastewater*. Nashville: Archea Press.

Tumutegyereize, P., Mugenyi, R., Ketlogetswe, C., & Gandure, J. (2016). A comparative performance analysis of carbonized briquettes and charcoal fuels in Kampala-urban, Uganda. *Energy for Sustainable Development, 31*, 91–96. https://doi.org/10.1016/j.esd.2016.01.001.

Walla, C., & Schneeberger, W. (2008). The optimal size for biogas plants. *Biomass and Bioenergy, 32*(6), 551–557. https://doi.org/10.1016/j.biombioe.2007.11.009.

Zaher, U., Li, R., Jeppsson, U., Steyer, J.-P., & Chen, S. (2009). GISCOD: General integrated solid waste co-digestion model. *Water Research, 43*(10), 2717–2727. https://doi.org/10.1016/j.watres.2009.03.018.